66. Fundamental Aspects of Ionic Dissociations: The Fragmentation Pathways of Excited Bicyclobutane Cations

by **Rolf Bombach, Josef Dannacher** and **J.-P. Stadelmann**

Physikalisch-Chemisches Institut der Universität Basel, Klingelbergstrasse 80, CH-4056 Basel

and **Reinhard Neier**

Institut de chimie organique, Université de Fribourg, Pérolles, CH-1700 Fribourg

In memorial of Henry M. Rosenstock (1927-1982)

(22.XI.82)

Summary

A most recently developed method to quantify the fragmentation pathways of excited radical cations is presented. Using bicyclobutane cation as an illustrative example, the RRKM analysis of the breakdown diagram determined by He-Iα photoelectron-photoion coincidence spectroscopy is outlined. The results imply complete isomerization to 1,3-butadiene cation preceding the dissociative processes. The rate-energy functions of four competitive primary fragmentation reactions, leading to $C_3H_3^+$, $C_4H_5^+$, $C_4H_4^+$ and $C_2H_3^+$ are established. There is compelling evidence that the production of $C_2H_4^+$ fragment ions does not compete effectively with these four reactions. The extent of kinetic and competitive shift effects is determined. The derived enthalpies of formation are in excellent accord with the available high quality reference data. The relative importance of different fragmentation pathways which ultimately lead to fragment ions of identical mass to charge ratio is assessed.

Introduction. – Molecular cations in various electronic states are formed when gaseous organic molecules are photoionized by He-Iα resonance radiation. Ample information about the basic nature of these initially populated electronic states, the partial photoionization cross sections and the corresponding ionization energies can usually be obtained from photoelectron spectroscopy. However, this extremely valuable technique is rather mute as far as the subsequent deactivation processes of the molecular ions are concerned. Relying on mass spectrometric means, the commonly prevailing relaxation mechanism of excited organic radical cations, *i.e.* radiationless transitions followed by dissociations into the energetically accessible fragmentation channels, can be probed on a very basic level by determining the mass to charge ratio and the relative abundance of the ions observed. A superior way to explore the dissociative processes involved is photoelectron-photoion coin-

cidence spectroscopy [1]. Since this method fully exploits the time-correlation between the detection of a particular photoelectron and the detection of the photoion stemming from the same ionization event, the behaviour of molecular cations can be studied as a function of their internal energy. The outcome of such a coincidence study, termed breakdown diagram of the molecular cation in question, quantifies the fragmentation products formed when parent ions with selected amounts of internal energy dissociate. The crucial pieces of information contained in the breakdown diagram are the rates of the various decay processes involved as a function of the available energy.

In order to gain the rate-energy dependencies of the dissociative steps, the effective sampling function and the time scale of the experiment have to be taken into account. In addition some simplifying assumptions are required, as we currently lack a feasible way to treat the most general case of a couple of fragmentations, each preceded by radiationless transitions, possibly accompanied by extended isomerizations, and perhaps even occurring on distinct electronic manifolds. Following the statistical theory of unimolecular reactions [2], it is therefore presupposed that any kind of excitation energy is degraded rapidly into internal energy of the electronic ground state, where it is completely randomized among the various internal degrees of freedom. This randomly distributed internal energy becomes the necessary and sufficient criterion for reaction and the fragmentations involved are considered as a number of competitive unimolecular processes taking place on a single electronic hypersurface. The energy dependence of the unimolecular rate constants of the individual fragmentations can then be derived from the experimental breakdown diagram. Adopting a suitable model function forthcoming from transition-state theory [2], the 0 K threshold energies of the processes can be determined and the bonding properties of the corresponding transition states can be characterized.

The most pertinent studies where photoelectron-photoion coincidence spectroscopy and transition-state theory have been combined on mutual terms, as outlined above, are of recent date [3]. Hitherto, these investigations had been confined to cases where the least endothermic dissociation is clearly separated in energy from higher energetic processes. Since molecular ions of more than ten atoms were singled out and the activation energies involved were larger than 2 eV, low threshold rates and unimolecular rate constants rising only slowly with increasing internal energy could be expected. This results in an extended internal energy range on the order of 0.5–1.0 eV where the unimolecular rate constant assumes values between 10^3 and $10^6\ s^{-1}$, which can be determined absolutely by coincidence spectroscopy. Such relatively small rate constants give rise to a dependence of the breakdown diagram on the experimental sampling time, which in its turn can be varied within a certain range, limited by the details of the experimental setup. Already a partial analysis of this time dependence is sufficient to derive the threshold energy of the process and to obtain a measure for the degree of bonding in the transition state [3]. With the help of a two-parameter-model function adopted from transition-state theory, this method has most lately been elaborated by making use of a complete analysis of an unusually extended experimental data set, gained for the decay of iodobenzene cation into phenyl cation plus iodine radical [4]. A remarkable

degree of accord was observed between measured and computed rates, even though the experimental data stemmed from three distinct coincidence spectrometers with clearly different inherent properties. In order to deduce the threshold energy of this reaction the model function was used to extrapolate the experimental rate-energy function down to threshold. The derived value for the threshold energy was in very good accord with the best thermochemical reference data available.

Most recently, the expounded procedure has been extended successfully to treat several competing unimolecular reactions [5]. The four lowest-energetic fragmentation processes of 1,3-butadiene cation have been investigated over an internal energy range of almost 2 eV. Excellent agreement between calculated and experimental data was obtained, indicating that a useful extrapolation of the method to higher excitation energies is feasible. Most notably, the reported discrepancy between experimental and theoretical results [6] could be removed. Additionally, the extent of kinetic and competitive shift effects was quantified and the lack of effective competition between $C_2H_4^+$ formation and the three reaction pathways leading to $C_3H_3^+$, $C_4H_5^+$ and $C_4H_4^+$ was uncovered. Although the absolute values for the total dissociation rate constants of 1,3-butadiene cation and four of its isomers, derived in an earlier coincidence study [6], were falsified due to the use of an incorrect sampling function [7]; another important result of that study [6] is not in doubt. It concerns the fact that the measured decay rates are independent of the structure of the molecular precursor for excess energies not exceeding the lowest fragmentation onset by more than 0.5 eV. This implies extended isomerizations among the different $C_4H_6^+$-isomers in the studied energy range, as was also found for other isomeric systems of hydrocarbon cations [8].

In the present study the fragmentation pathways of a further $C_4H_6^+$-isomer, *i.e.* bicyclobutane cation, are investigated. A comparison of the breakdown diagram of this species with the breakdown diagram of 1,3-butadiene cation [9] can immediately reveal the degree of isomerization to common precursor structures. However, based on classical kinetics data for the isomerization of the corresponding neutrals [10] distinct behaviour of the two isomers could be expected, at least for very small excess energies above the lowest fragmentation threshold. Moreover, it was tempting to use the developed model to probe the importance of different pathways leading to fragment ions of identical mass to charge ratio.

Results and discussion. – The photoelectron spectrum of bicyclobutane shows five clearly separated bands between 8 and 18 eV *(cf. Fig. 1)*. Adopting the assignment of the spectrum proposed in [11], seven electronic states of the bicyclobutane radical cation are populated in this energy range falling to the share of these five bands, as summarized in *Table 1*. Note that the ionization process leading to the electronic ground state of the radical cation involves the ejection of a photoelectron from the molecular orbital essentially located in the transannular σ-bond [11]. The position of the onset of band ① suggests an adiabatic ionization energy of $I = 8.70 \pm 0.02$ eV. This value is of particular importance, because the unimolecular rate constant depends strongly on the activation energy, which is measured relative to the vibronic ground state of the reactant. Therefore, this quantity has been redetermined independently using threshold photoelectron spectroscopy [12].

Table 1. *Ionization energies of bicyclobutane and the electronic states of its radical cation populated upon He-Iα photoionization*[a])

PE.-band	State	Symmetry[b])	Ionization energy (eV)[c])
①	$\tilde{X}$	$^2A_1$	8.70 ± 0.02[d])
			9.25 ± 0.05
②	$\tilde{A}$	$^2A_2$	11.5 ± 0.3
	$\tilde{B}$	$^2B_2$	
③	$\tilde{C}$	$^2B_1$	13.00 ± 0.05
④	$\tilde{D}$	$^2A_1$	14.50 ± 0.05
	$\tilde{E}$	$^2B_2$	
⑤	$\tilde{F}$	$^2A_1$	16.90 ± 0.02[e])
			17.05 ± 0.02

[a]) Assignment adopted from [11]. [b]) C_{2v}-point group. [c]) This work, position of the band maxima. [d]) This work and [12]; onset of band ① accepted as adiabatic ionization energy of bicyclobutane. [e]) Adiabatic ionization energy of the $\tilde{F}$ ($^2A_1$) state.

These latter experiments led to an identical value of $I = 8.700 \pm 0.005$ eV for the onset of band ①.

The mass spectral data collected in *Table 2* evidence that He-Iα photoionization of bicyclobutane yields stable as well as dissociating molecular ions. The principally conceivable fragmentation pathways leading to the seven distinct product ions of significant (> 0.05) relative intensity are depicted in *Scheme*. Note that the molecular ion in question is of relatively small size and only moderately excited. Moreover, only very few different product ions are observed. Nevertheless, the present

Table 2. *Mass spectral data for bicyclobutane*

m/z	PI.[a])	EI.[b])	
	21.22 eV	21 eV	75 eV
55	4.5	4.5	4.5
54	100	100	100
53	80	56	71
52	13	6	11
51	22	7	22
50	2	2	15
49			5.5
48			1
40	2.5	3	2.5
39	83	86	68
38	2	2	5
37			3
29	1	1	1
28	41	25	31
27	65	16	40
26	6	3	11
25.5			2
25			1

[a]) This work, He-Iα photoionization, *Balzers QMG-511*. [b]) This work, *Hitachi-Perkin-Elmer RMU-7D*, 5 μA emission current.

Scheme

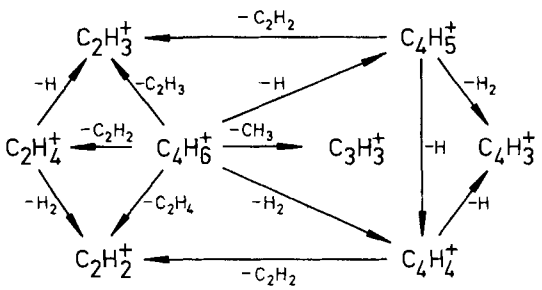

example already illustrates the two most important complications emerging when the statistical theory of unimolecular reactions (originally developed for the field of classical kinetics) is used to analyze experimental data on ionic fragmentations. Firstly, a ramified system of parallel and consecutive reactions leads to an intricate kinetics. Secondly, the further decay of sufficiently excited daughter ions poses

Table 3. *Reaction pathways i=(1)-(13) and their respective 0 K threshold energies of bicyclobutane molecular cation*[a])

Reaction number	Reaction	Calculated threshold energy [eV]
1	$C_4H_6^+ \xrightarrow{k^{(1)}} C_4H_4^+ + H_2$	9.98
2	$\xrightarrow{k^{(2)}} C_3H_3^+ + CH_3$	10.12
3	$\xrightarrow{k^{(3)}} C_4H_5^+ + H$	10.28
4	$\xrightarrow{k^{(4)}} C_2H_4^+ + C_2H_2$	11.07
5	$\xrightarrow{k^{(5)}} C_2H_3^+ + C_2H_3$	11.94
6	$\xrightarrow{k^{(6)}} C_2H_2^+ + C_2H_4$	11.97
7	$\longrightarrow (C_4H_5^+ + H) \xrightarrow{k^{(7)}} C_4H_3^+ + H_2 + H$	13.09
8	$\longrightarrow (C_4H_4^+ + H_2) \xrightarrow{k^{(8)}} C_4H_3^+ + H + H_2$	13.09
9	$\longrightarrow (C_4H_4^+ + H_2) \xrightarrow{k^{(9)}} C_2H_2^+ + C_2H_2 + H_2$	13.69
10	$\longrightarrow (C_2H_4^+ + C_2H_2) \xrightarrow{k^{(10)}} C_2H_2^+ + H_2 + C_2H_2$	13.69
11	$\longrightarrow (C_4H_5^+ + H) \xrightarrow{k^{(11)}} C_2H_3^+ + C_2H_2 + H$	13.83
12	$\longrightarrow (C_2H_4^+ + C_2H_2) \xrightarrow{k^{(12)}} C_2H_3^+ + H + C_2H_2$	13.83
13	$\longrightarrow (C_4H_5^+ + H) \xrightarrow{k^{(13)}} C_4H_4^+ + H + H$	14.46

[a]) These values have been calculated using the thermochemical data collected in *Table 4.*

additional questions concerning the partition of the excess energy available for the primary reaction. In the present context we face the problem to assess the relative importance of a series of thirteen unimolecular dissociations, arranged in order of increasing threshold energies in *Table 3.*

It is important to note that only the first six reactions are primary processes of the molecular ion, while the remaining seven fragmentations reflect dissociations of first generation daughter ions. Since the rate of a unimolecular reaction rises generally very steeply with increasing excess energy, the decay of the first generation daughter ion represents the rate-determining step of processes 7–13. In view of the complications originating in the presence of these consecutive processes our analysis will first be confined to ionization energies not exceeding 13 eV. A reliable extension to higher energies can later be attempt if the energy dependence of the rate constants of the primary processes ($k^{(1)}$–$k^{(6)}$) has been determined for $I < 13$ eV.

The primary fragmentation pathways at low excitation energies of the parent ion ($I < 13$ eV). The details of coincidence data evaluation have been discussed extensively in several earlier studies [13]. The breakdown diagram of bicyclobutane cation is presented in *Figure 1.* As an illustration we note that the fragmentations of bicyclobutane cations with an internal energy of $E^* = 4.3$ eV ($I \approx 13$ eV) lead to the following product distribution: $C_4H_5^+$ (0.40), $C_3H_3^+$ (0.30), $C_2H_4^+$ (0.26), $C_4H_4^+$ (0.04). The noteworthy features of the low energy ($I < 13$ eV) section of the breakdown diagram of bicyclobutane cation can quickly be enumerated. Firstly, there are no dissociative processes below $I = 10$ eV. Therefore, with the exception of the most highly excited vibrational levels populated, He-Iα photoionization to the electronic ground state leads to molecular ions which are stable on the time scale of the experiment. Secondly, the formation of $C_3H_3^+$ and $C_4H_5^+$, is observed at $I = 10.0$–10.5 eV. In this energy range, some undissociated molecular ions are still detected, as evidenced by the fact, that the branching ratios of the two product ions do not add up to unity. A partial analysis of this energy span where parent and daughter ions are detected shows, that the threshold rates involved are on the order of $10^3\ s^{-1}$. Thirdly, above 10.5 eV no molecular ions are detected and the formation of two further dissociation products, $C_2H_4^+$ and $C_4H_4^+$ is observed. Fourthly, the directly apparent threshold energies for the reactions 2, 3 and 4 are close to the calculated values, whereas there is a striking difference of ≈ 2 eV between calculated and apparent threshold in the case of reaction 1. Furthermore, though energetically possible, the formation of $C_2H_3^+$ and $C_2H_2^+$ is not detected at $I < 13$ eV.

The breakdown diagram of a molecular ion can in principle be calculated relying on the statistical theory of unimolecular reactions [2] and adopting the additional assumptions which have been summarized in the introduction of the present article. The essential quantities required in practice to calculate the corresponding unimolecular rate constants as a function of the available excess energy are the activation energies of the processes and a set of frequencies for the reactant as well as the transition states. Currently, an exact determination of these quantities is generally not feasible and, thus, one is forced to work with suitable approximations. A practicable and consistent way which has lately been developed [3–5] can be characterized as follows. Unless definite information to the contrary is available

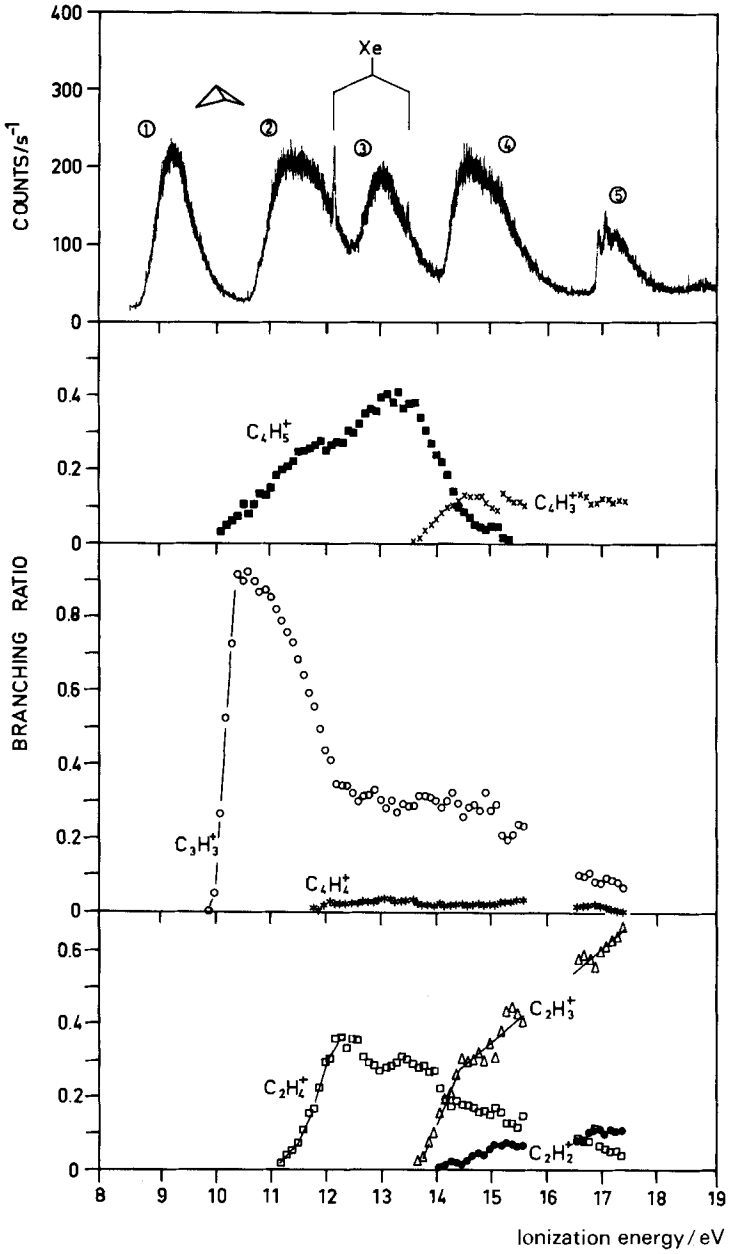

Fig. 1. *The photoelectron spectrum of bicyclobutane and the experimentally determined breakdown diagram of its radical cation.* As a consequence of the very low electron intensity, coincidence measurements around $I = 16$ eV are not feasible.

it is assumed that the dissociations take place on the ground-state hypersurface of the molecular ion in question and the corresponding frequencies are equated to their neutral counterparts. Appropriate internal degrees of freedom [2] are defined as reaction coordinates and assigned to each fragmentation. The frequencies of each transition state are approximated by the respective molecular values altered by a constant factor $F^{(i)}$. Using the activation energies $E_0^{(i)}$ and these factors $F^{(i)}$ as the only adjustable parameters, a standard regression technique is employed to fit calculated model functions of the form

$$k^{(i)}(E^* - E_0^{(i)}) = \sigma^{(i)} \frac{W^{\neq (i)}(E^* - E_0^{(i)})}{h \cdot \rho(E^*)}$$

to the experimental data. Letter i identifies the various reactions and $\sigma^{(i)}$ denotes the corresponding reaction-path degeneracies [2]. E^*, $E_0^{(i)}$, $\rho(E^*)$ and $W^{\neq (i)}(E^* - E_0^{(i)})$ represent, respectively, the available excess energy, the critical energy of *reaction i*, the density of states of the precursor with internal energy E^* and the integrated density of states of the transition state of *reaction i*, taken between threshold and $(E^* - E_0^{(i)})$. Several independent studies have shown [3–5] that good accord between theory and experiment can be achieved and that reliable values for the activation energies can be obtained even when the thresholds are experimentally inaccessible. Moreover, the computed $F^{(i)}$-values represent a useful indicator for the presence of particularly loose or tight transition states.

Two noteworthy difficulties emerged when this method was applied to analyze the present data. To begin with, it was realized that a bicyclobutane cation structure of the precursor ion could never account for the measured threshold rates. According to the statistical theory of unimolecular reactions [2], the unimolecular rate constant is a monotonous function of the excess energy E^*, assuming its minimum value, $k_{min} = \sigma/h \cdot \rho(E^*)$, at threshold. Assigning a bicyclobutane cation structure to the reactant results in $k_{min} > 10^6$, which exceeds the experimental values by more than three orders of magnitude. Referring to a particular elementary composition of the reactant, $\rho(E^*)$ is essentially given by the activation energy of the process and is, comparably, only slightly affected by the distinct sets of frequencies belonging to the normal modes of the different isomers. In the present case, only the most stable $C_4H_6^+$-isomer, *i.e.* 1,3-butadiene cation, provides an activation energy high enough to account for the experimental rates. Consequently, an isomerization of bicyclobutane cation to 1,3-butadiene cation preceding the fragmentation has to be postulated. Accordingly the vibrational frequencies of neutral 1,3-butadiene [14] have been employed for the reactant and, after multiplication with $F^{(i)}$, also for the transition states. Since this isomerization appears to be complete at the threshold energy of the lowest energy process (see below), a 0 K activation energy of at most 137 kJ mol^{-1} is implied, which is significantly lower than the barrier (171.5 kJ mol^{-1} [10]) for the isomerization of the corresponding neutrals.

The second difficulty encountered at the outset of our analysis concerns the formation of $C_2H_4^+$-fragment ions. All attempts failed to include *process 4* as a further fragmentation competitive with the three lowest energetic *reactions 1, 2* and *3*, as a consequence of the following reasons. The experimental threshold for

$C_2H_4^+$ formation *(cf. Fig. 1)* exceeds the dissociation limit associated with *reaction 4* by merely 0.1 eV. Referring to the concept of minimum rate [2] and to a 1,3-butadiene structure of the reactant the rate at the thermochemical dissociation limit ($I = 11.07$ eV) for the production of $C_2H_4^+$ is $k^{(4)} \approx 1\ s^{-1}$, whereas $k_{TOT} = \Sigma_i k^{(i)} \cong 10^7\ s^{-1}$ at this very energy (see below). Therefore, within 0.1 eV, $k^{(4)}$ has to increase by about five orders of magnitude to account for the 1% $C_2H_4^+$ branching ratio at $I = 11.2$ eV (see *Fig. 1*). Such an enormeous increase can hardly be produced at all and would imply an absolutely unrealistically loose transition state. However, even if this huge increase could be accomplished the problem would not be solved, because $k^{(4)}$ would continue to rise extremely steeply and, thus, quench the other fragmentations completely, little above the threshold energy of *reaction 4*. Accordingly, it is concluded that $C_2H_4^+$-formation is not in effective competition with the *reactions 1, 2* and *3*. Therefore, the coincidence data had been renormalized neglecting the parent ions which dissociate according to *reaction 4* and the corresponding secondary fragmentation products (see below).

When the analysis is confined to the competitive formation of $C_3H_3^+$-, $C_4H_5^+$- and $C_4H_4^+$-fragment ions, the calculated rate constants yield a breakdown diagram according to the dashed lines in *Figure 2*. Allowing for the margins of error of the experimental results (typical relative errors of the branching ratios are on the order of 5–10%) the agreement between calculated and measured data is rather good. Substantial discrepancies emerge, if the calculated values are extrapolated to significantly higher energies. Considering $C_4H_5^+$ and $C_4H_4^+$ the disparity could be assigned to secondary dissociations, since the calculated branching ratios exceed the measured ones. However, there are no secondary decay processes diminishing the $C_3H_3^+$ branching ratio at higher energies.

Table 4. *Relevant thermochemical data*[a])

Neutral				Cation	
	$\Delta_f H^\ominus_{0(g)}$	$\Delta_f H^\ominus_{298(g)}$	Ionization energy	$\Delta_f H^\ominus_{0(g)}$	$\Delta_f H^\ominus_{298(g)}$
C_4H_6[b])	234.2[c])	217.2[d])	8.70[e])	1073.6	1056.6
C_4H_6[f])	123.6[g])	108.8[d])	9.06	997.8	983.0
C_4H_5				1010.0[h])	1000.0[i])
C_4H_4				1195.0[j])	1185.0[i])
C_4H_3				1281.0[k])	1271.0[l])
C_3H_3[m])				1065.0[h])	1055.0[i])
C_2H_4	60.7	52.3	10.51	1075.0	1066.6
C_2H_3	261.5	257.0[i])	8.95	1125.0	1120.5
C_2H_2	227.3	226.7	11.41	1328.0	1327.4
CH_3	145.6	142.3			
H	216.0	218.0			

[a]) Data drawn from [21] in the absence of other citations. Enthalpies in kJ mol^{-1} and ionization energies in eV. [b]) Bicyclobutane. [c]) Conversion of the corresponding 298 K value to 0 K using the vibrational frequencies given in [22] and the approximate enthalpy function of [23]. [d]) See [24]. [e]) This work and [12], see also *Table 1*. [f]) 1,3-Butadiene. [g]) Analogous to footnote c using the vibrational frequencies of 1,3-Butadiene given in [14]. [h]) See [5]. [i]) Estimated from the corresponding 0 K-value. [j]) See [3]. [k]) Estimated from the corresponding 298 K-value. [l]) See [25]. [m]) Cyclopropyl radical.

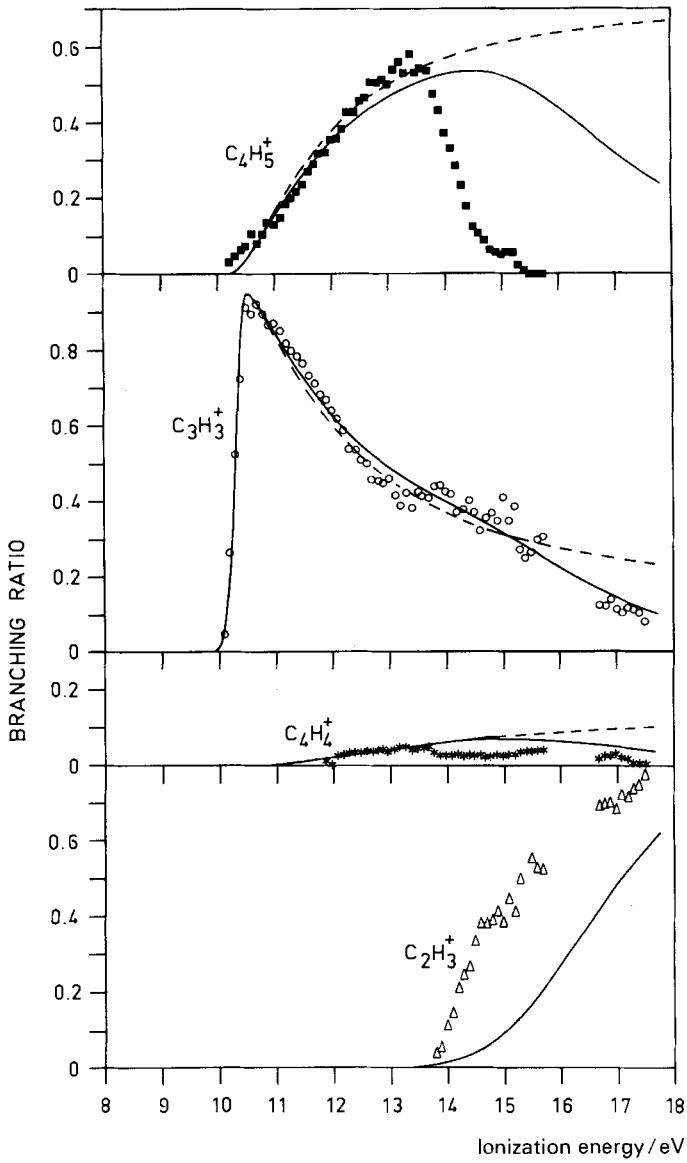

Fig. 2. *The renormalized breakdown diagram including only the four competitive primary fragmentations* (see text) *and the best fits to these data* (solid lines). The dashed lines are the results of a preliminary model which includes only three competitive reactions.

The only way to remove the discrepancy is to include a further competitive fragmentation pathway, which by necessity must be *reaction 5*. This approach affects the low energy results ($I < 15$ eV) only slightly and yields the desired change of the $C_3H_3^+$ breakdown curve at higher energies (see solid line in *Fig. 2*). Addi-

tionally $E_0^{(5)}$ is in very good agreement with independent thermochemical data and $F^{(5)}$ implies the expected loose transition state for this process (see below).

The thermochemical and kinetic parameters obtained in the course of our analysis are summarized in *Table 5*. The enthalpies of formation derived for the $C_3H_3^+$-, $C_4H_5^+$- and $C_2H_3^+$-fragment ions agree pleasingly well with the known thermochemistry of these ions. Our data indicate a substantial activation energy of

Table 5. *Energetic and kinetic parameters derived from the coincidence data*

Reaction number (i)	Ionic fragment	$E_0^{(i)}$ (eV) [a]	0 K-threshold energy (eV) [b]	$\Delta_f H^{\ominus}_{0(g)}$ (kJ mol^{-1}) [c]	$F^{(i)}$ [d]	$S^{\neq}_{1000\,K}$ (cal deg^{-1}) [e]	$A_{1000\,K}$ (s^{-1}) [f]	$A_{classical}$ (s^{-1}) [g]
1	$C_4H_4^+$	2.70	10.61[h]	1258[i]	1.080	−2.33	$1.8 \cdot 10^{13}$	$1.6 \cdot 10^{13}$
2	$C_3H_3^+$	2.21	10.12[j]	1065	1.035	−2.60	$1.5 \cdot 10^{13}$	$1.6 \cdot 10^{13}$
3	$C_4H_5^+$	2.42	10.33[j]	1015	1.005	−0.42	$4.6 \cdot 10^{13}$	$8.3 \cdot 10^{13}$
5	$C_2H_3^+$	3.95	11.86[h]	1117	0.745	9.34	$6.2 \cdot 10^{15}$	$3.1 \cdot 10^{16}$

[a]) 0 K-critical energy of *reaction i*, referring to the vibronic ground state of 1,3-butadiene cation, see text. [b]) Calculated from the $E_0^{(i)}$-values and the thermochemical data listed in *Table 4*. [c]) This work. [d]) Frequency multiplier for the transition states, see text. [e]) Equivalent formal activation entropy at 1000 K, see [2]. [f]) Equivalent preexponential factor at 1000 K, see [2]. [g]) Equivalent classical preexponential factor, see [2]. [h]) ±0.2 eV, error limits derived from the estimated standard errors deduced from the fitting procedure. [i]) Contains the reverse activation energy, see text. [j]) ±0.1 eV, error limits derived from the estimated standard errors deduced from the fitting procedure.

≈0.6 eV for the reverse process of *reaction 1*, in quantitative accord with the outcome of a similar analysis of the fragmentation of 1,3-butadiene cation [5]. The presence of such a barrier is not unexpected for the elimination of a hydrogen molecule [15]. According to our $F^{(i)}$ values and the formally derived activation entropies, the transition states for i = 1,2,3 appear to be tighter than the reactant. This can be ascribed to the formation of a three membered ring required to form the corresponding fragments at threshold [8]. On the other hand, the transition state for *reaction 5* is loose implying a simple bond breaking process. Inserting the best fit parameters given in *Table 5*, the individual rate energy functions of the four *dissociations 1, 2, 3* and *5* can be computed (see *Fig. 3*). Referring to the time scale of our experiment and the determined threshold rates, it is obvious that kinetic shift effects are fairly small. Consequently, the apparent onset of the breakdown curves of $C_3H_3^+$ and $C_4H_5^+$ are useful estimates for the threshold energies of these processes. In contrast, the observed onsets for $C_4H_4^+$- (I = 11.8 eV and $C_2H_3^+$- (I = 13.8 eV) formation are meaningless quantities as considerable competitive shifts [16] are operating. It is recalled, that a kinetic shift originates ultimately in low absolute values of the total fragmentation rate constant k_{TOT}, while a competitive shift emerges when the rate of a particular dissociation is small relative to k_{TOT}. We wish to point out that the outlined method provides reliable values for the threshold energies even when kinetic- and/or competitive shift effects are present.

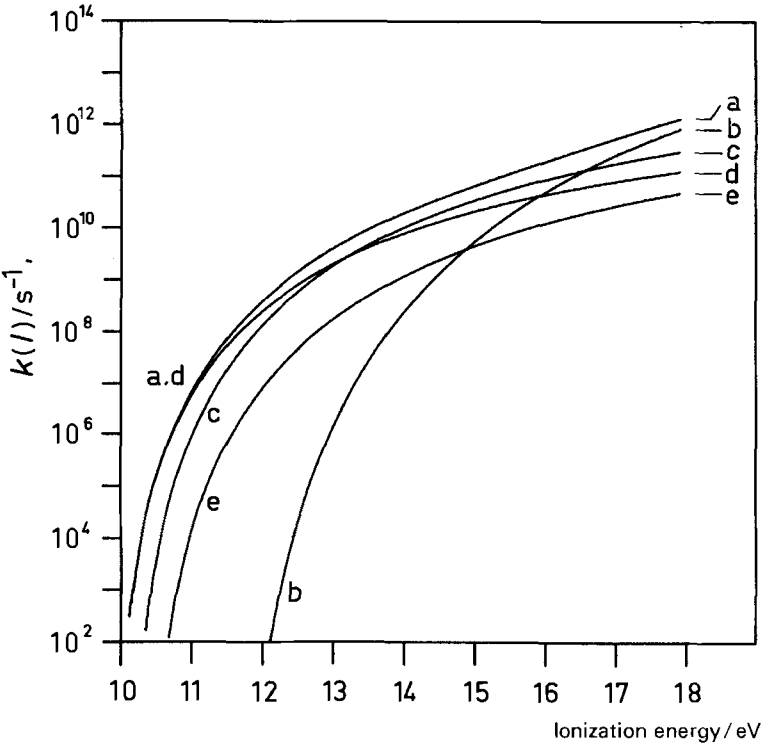

Fig. 3. *The rate-energy functions of* processes 2 *(d)*, 3 *(c)*, 1 *(e)* and 5 *(b)* as well as the energy dependence of the total rate *(a)*

The fragmentation pathways at high excitation energies of the parent ion ($I > 13$ eV). – Our more qualitative description of the relative importance of the high-energy-fragmentation pathways starts advantageously with a discussion of *reaction 4* and the consecutive decay processes of the ethylene cation, *i.e. reactions 10* and *12*. Referring to the explored ionization energy range of the bicyclobutane cation, the first generation $C_2H_4^+$-daughter ion can contain up to 6.4 eV of internal energy. The breakdown diagram of ethylene cation has been determined by threshold photoelectron-photoion-coincidence spectroscopy [17]. These measurements have shown, that ethylene cations possessing less than 2.7 eV of internal energy do not fragment. Consequently, the variation of the branching ratio of the $C_2H_4^+$-fragment ions formed according to *reaction 4* cannot be related to the presence of secondary decay processes for $I \leqslant 13.8$ eV. Following reference [17], the $C_2H_4^+$-ions decay rapidly by loss of a hydrogen molecule or by abstraction of a hydrogen radical, when their internal energy assumes values between 2.7 and 7.5 eV. In order to gain the rate energy dependencies of these two fragmentations of the ethylene cation, the breakdown diagram reported in reference [17] has been analyzed [18] using the approach outlined above. The derived values for the parameters are in good accord with the available literature data and the two processes appear to compete effectively on the ground state manifold of the ethylene cation. The agreement

between the experimental [17] and the computed [18] breakdown curves is remarkable *(cf. Fig. 4)* providing further evidence for the reliability of our method.

It is important to realize that the internal energy of the $C_2H_4^+$-product ions formed in *reaction 4* is not *a priori* determined, even when these ions stem originally from internal energy selected bicyclobutane cations. Any available excess energy of the precursor fragmenting according to *reaction 4* is partitioned among the external and internal degrees of freedom of the charged and the neutral fragment. There is no indication for a large kinetic energy release in the case of *reaction 4* and rotational excitation of the separating fragments is usually small. In order to estimate the internal energy of those $C_2H_4^+$-ions which are sufficiently excited to undergo a secondary decay, it is assumed that the excess energy is partitioned statistically [2] [19] between the internal degrees of freedom of the $C_2H_4^+$-ion and

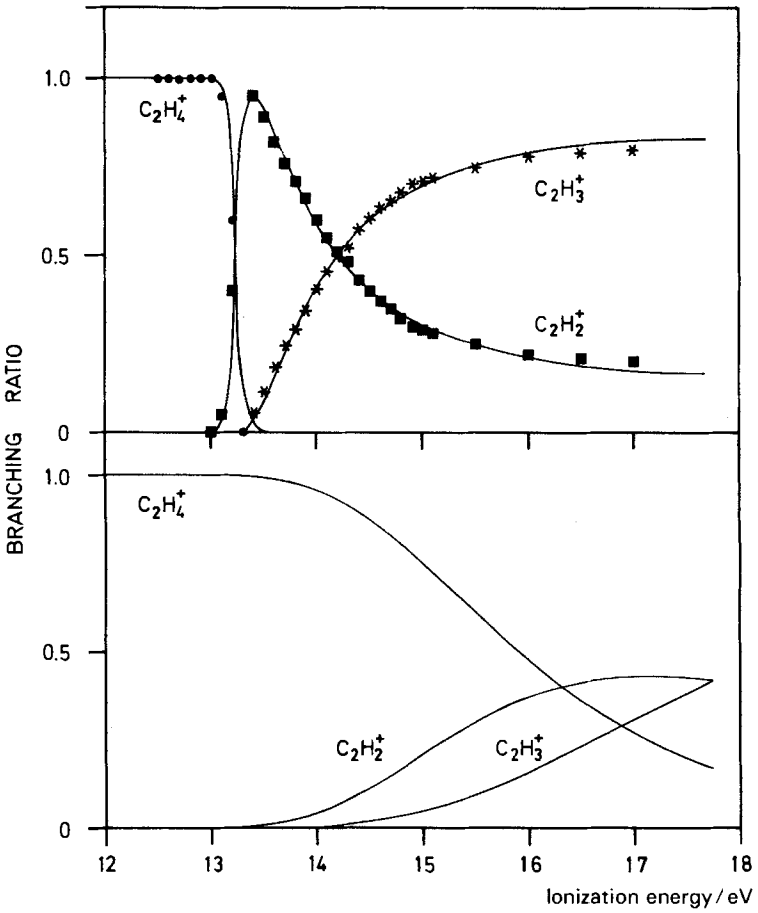

Fig. 4. Top: *Calculated* [18] *and experimental* [17] *breakdown diagram of internal energy selected ethylene cations.* Bottom: *The breakdown diagram of ethylene cation calculated assuming broad internal energy distribution in course of* reaction 4.

the C_2H_2 neutral. The problem is then reduced to enumerate the number of ways n quanta of energy can be distributed among two degenerate harmonic oscillators of frequency ν. In the present context we have set $\nu \triangleq 0.2$ eV and assigned degeneracies of 12 and 7 to $C_2H_4^+$ and C_2H_2, respectively. Referring to a particular excess energy of $E^{(4)}_{excess} \triangleq n \cdot \nu$ the probabilities for finding a given number of quanta in the $C_2H_4^+$ ion are depicted in *Figure 5*. The two examples shown are smooth curves

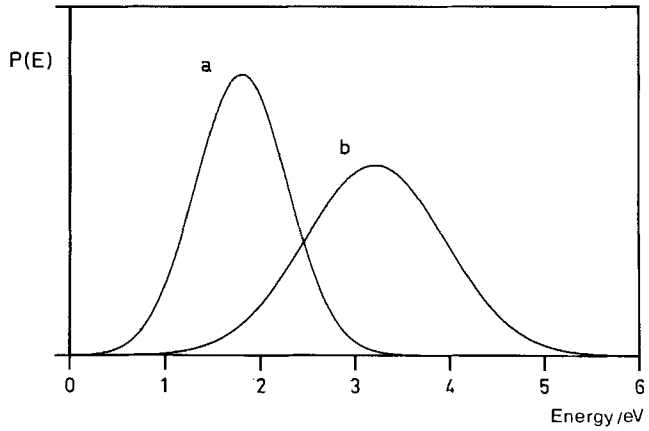

Fig. 5. *The normalized probability P(E) that a particular energy is found in the $C_2H_4^+$-fragment ion, when the excess energy of* reaction 4 *amounts to 3.4 eV (a) or 5.4 eV (b)*

for n = 17 and n = 27, revealing that the $C_2H_4^+$-ions involved in *reactions 10* and *12* can contain strongly different amounts of internal energy for a given value of $E^{(4)}_{excess}$. The correspondingly broadened effective sampling function effaces most of the dominant features of the breakdown diagram of internal energy selected ethylene cations (see *Fig. 4*, bottom). Based on these considerations the declining part of the $C_2H_4^+$-breakdown curve was calculated assuming a constant value of 0.25 for the branching ratio of the primary $C_2H_4^+$ daughter ion. The general shape of the computed curves accounts qualitatively for the measured values *(cf. Fig. 6)*. The analysis suggests, that the majority of the acetylene cations observed in the He-Iα photoionization mass spectrum of bicyclobutane is formed in the course of *reaction 10*. Some $C_2H_2^+$-ions may be produced in *reaction 9*, while $k^{(6)}$ is estimated to be too small to compete effectively with the other primary processes.

There is no doubt, that the difference between the calculated and the measured breakdown-curve for $C_4H_5^+$ at $I > 13.75$ eV originates in secondary reactions of this ion. Compared with the ethylene cations, the internal energy distribution of the $C_4H_5^+$-fragment ions is much narrower, because the neutral fragment of *reaction 3* has no internal degrees of freedom. This results in a much steeper decrease of the breakdown curve of the $C_4H_5^+$ primary daughter ions *(cf. Fig. 2)*. The relative importance of the three (*reactions 7, 11* and *13*) accessible secondary dissociations of the $C_4H_5^+$-ions can be estimated as follows. There are three different processes leading to $C_2H_3^+$-fragment ions. The contributions of *reaction 12* have been sub-

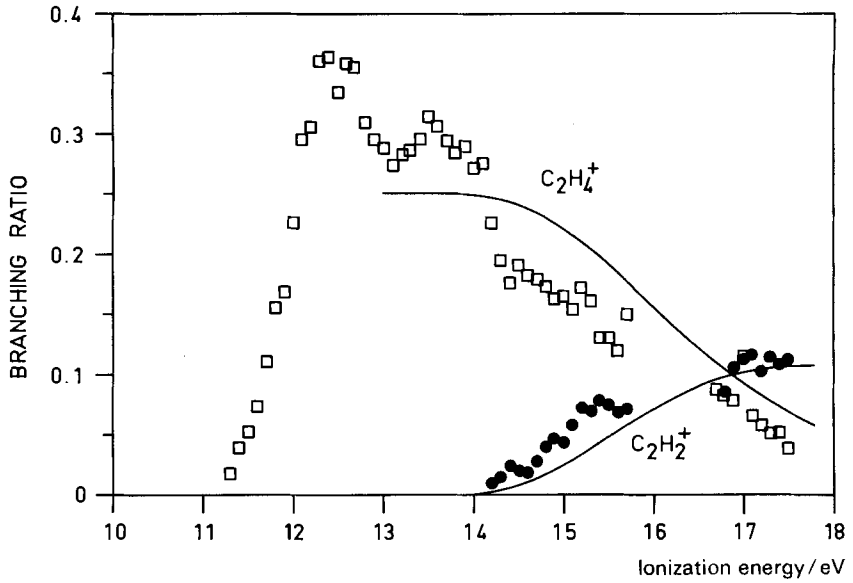

Fig. 6. *The experimental breakdown curves for $C_2H_4^+$ and $C_2H_2^+$, and the calculated breakdown curves for the secondary decay of $C_2H_4^+$ into $C_2H_2^+ + H_2$*

tracted from the $C_2H_3^+$-breakdown curve before renormalizing the data since the corresponding primary process does not compete with the other fragmentation pathways (see above). The calculated $C_2H_3^+$-breakdown curve given in *Figure 2* represents the share stemming from *reaction 5*. Therefore, the difference between the experimental and the calculated $C_2H_3^+$-breakdown curve must be due to *reaction 11*. However, this channel alone cannot account for the observed decrease of the breakdown curve of the $C_4H_5^+$-ions. In view of the significantly different threshold energies and the magnitude of the respective branching ratios we conclude that the remaining $C_4H_5^+$-decay preferentially through *reaction channel 7* and only to a very small extent according to *reaction 13*. Calculated and experimental $C_4H_4^+$-breakdown curve coincide up to $I = 13.7$ eV (see *Fig. 2*). The adjacent decrease of the experimental breakdown curve can be ascribed to *reactions 8* and *9*. The internal energy distribution of the $C_4H_4^+$ primary daughter ions is expected to be somewhat broader than those of the $C_4H_5^+$-ions due to the presence of an activation energy for the reverse *reaction 1* and as a consequence of the internal degree of freedom of the neutral fragment formed in *reaction 1*. Nevertheless, the $C_4H_4^+$-breakdown curve would be expected to vanish at $I \leqslant 15$ eV. The detection of stable $C_4H_4^+$-ions at significantly higher energies indicates that *reaction 13* takes place, too.

Conclusions. – The present study reveals that even the seemingly simple PI mass spectrum of a rather small hydrocarbon is in fact the product of a complex scheme of unimolecular reactions. The details of these processes can be assessed

when the results of photoelectron-photoion coincidence spectroscopy are analyzed by a simple and consistent formulation of transition-state theory. The excellent agreement between experimental and calculated results obtained in several [3] [4] [5] [18] independent cases furnishes evidence of the reliability of our approach. The method renders it possible to determine the unimolecular rate constants as a function of the available excess energy. Moreover, reliable values for the threshold energies can be obtained even when considerable kinetic and/or competitive shift effects are present. The derived enthalpies of formation are in very good agreement with high quality reference data. The lack of reaction competition can be established in favourable cases and the bonding properties of the transition states can be qualitatively characterized. Since a large energy range (≈ 10 eV) can be probed, the relative importance of a series of parallel and consecutive unimolecular reactions can be determined. Most notably, the contributions from different fragmentation pathways leading ultimately to product ions of identical mass to charge ratio can now be estimated.

The success of the approach gives reason to hope that the theory of mass spectra of organic molecules can be improved substantially. Furthermore we expect fundamental information on unimolecular reactions which is hardly obtainable from the field of classical kinetics.

This work is part C26 of project no. 2.017-081 of the *Schweizerischer Nationalfonds zur Förderung der wissenschaftlichen Forschung* (part C25, cf. [5]). The *Max-Geldner Stiftung*, Basel, is thanked for a grant and support by *Ciba-Geigy SA, F. Hoffmann-La Roche & Cie. SA* and *Sandoz SA* (Basel) is gratefully acknowledged.

Experimental. – Bicyclobutane was prepared according to the procedure described in [20]. The sample was purified by preparative gas chromatography. NMR.- Mass- and photoelectron spectrum showed that no significant amounts of impurities were present.

The details of the coincidence spectrometer used and the way of coincidence data evaluation are described extensively in reference [13].

REFERENCES

[1] *T. Baer*, in 'Gas Phase Ion Chemistry', M.T. Bowers (editor), Academic Press, New York (1979), Chapter 5.
[2] *W. Forst*, 'Theory of Unimolecular Reactions', Academic Press, New York and London (1973).
[3] *H.M. Rosenstock, R. Stockbauer & A.C. Parr*, Int. J. Mass Spectrom. Ion Phys. *38*, 323 (1981) and references therein.
[4] *J. Dannacher, H.M. Rosenstock, R. Buff, A.C. Parr, R.L. Stockbauer, R. Bombach & J.-P. Stadelmann*, Chem. Phys., (1983) in press.
[5] *R. Bombach, J. Dannacher & J.-P. Stadelmann*, J. Am. Chem. Soc., (1983) in press.
[6] *A.S. Werner & T. Baer*, J. Chem. Phys. *62*, 2900 (1975).
[7] *T. Baer*, private communication.
[8] *H.M. Rosenstock, J. Dannacher & J.F. Liebman*, Radiat. Phys. Chem. *20*, 7 (1982).
[9] *J. Dannacher, J.-P. Flamme, J.-P. Stadelmann & J. Vogt*, Chem. Phys. *51*, 189 (1980).

[10] *R. Srinivasan, A.A. Levi & I. Haller,* J. Phys. Chem. *69,* 1775 (1965); *H.M. Frey & I.D.R. Stevens,* Trans. Faraday Soc. *61,* 90 (1965).
[11] *R. Gleiter,* Topics in Current Chem. *86,* 197 (1979).
[12] *J. Dannacher,* unpublished results.
[13] *J.-P. Stadelmann,* Ph. D. Thesis, University of Basel, 1981; and references therein.
[14] *T. Shimanouchi,* Tables of Molecular Vibrational Frequencies, Vl. I, Natl. Std. Ref. Data Ser. 39 (1972).
[15] *R. Bombach, J. Dannacher, J.-P. Stadelmann & J. Vogt,* Chem. Phys. Lett. *76,* 429 (1980).
[16] *F.W. McLafferty, T. Wachs, C. Lifshitz, G. Innorta & P. Irving,* J. Am. Chem. Soc. *92,* 6867 (1970).
[17] *R. Stockbauer & M.G. Inghram,* J. Chem. Phys. *62,* 4862 (1975).
[18] *R. Bombach, J. Dannacher & J.-P. Stadelmann,* unpublished results.
[19] *L.S. Kassel,* The Kinetics of Homogeneous Gas Reactions, Chem. Catalog., New York 1932.
[20] *G.M. Lampman & J.C. Aumiller,* Org. Synth. *51,* 55 (1971).
[21] *H.M. Rosenstock, K. Draxl, B.W. Steiner & J.T. Herron,* J. Phys. Chem. Ref. Data 6, Suppl. 1 (1977).
[22] *I. Haller & R. Srinivasan,* J. Chem. Phys. *41,* 2745 (1964).
[23] *D.R. Stull & H. Prophet,* JANAF Thermochemical Tables, 2nd edn., NSRDS-NBS 37, U.S. Department of Commerce, June 1971.
[24] *K.B. Wiberg & R.A. Fenoglio,* J. Am. Chem. Soc. *90,* 3395 (1968).
[25] *J. Dannacher,* Chem. Phys. *29,* 339 (1978).